JOURNAL OF MATERIALS SCIENCE **36** (2001) 1411–1417

Modeling microarchitecture and mechanical behavior of nacre using 3D finite element techniques

Part I *Elastic properties*

DINESH R. KATTI*, KALPANA S. KATTI
Department of Civil Engineering, North Dakota State University, Fargo, ND 58105, USA
E-mail: Dinesh_Katti@Ndsu.Nodak.edu

Three dimensional finite element models of nacre were constructed based on reported microstructural studies on the 'brick and mortar' micro-architecture of nacre. 3D eight noded isoparametric brick elements were used to design the microarchitecture of nacre. Tensile tests were simulated using this model. The tests were conducted at low stresses of 2 MPa which occur well within the elastic regime of nacre and thus effects related to locus and extent of damage were ignored. Our simulations show that using the reported values of elastic moduli of organic (0.005 GPa) and aragonitic platelets (205 GPa), the displacements observed in nacre are extremely large and correspond to a very low modulus of 0.011 GPa. The reported elastic modulus of nacre is of the order of 50 GPa. The reason for this inconsistency may arise from two possibilities. Firstly, the organic layer due to its multilayered structure is possibly composed of distinct layers of different elastic moduli. The continuously changing elastic modulus within the organic layer may approach modulus of aragonite near the organic-inorganic interface. Simulations using variable elastic moduli for the organic phase suggest that an elastic modulus of 15 GPa is consistent with the observed elastic behavior of nacre. Another explanation for the observed higher elastic modulus may arise from localized platelet-platelet contact. Since the observed modulus of nacre lies within the above two extremes (i.e. 15 GPa and 205 GPa) it is suggested that a combination of the two possibilities, i.e. a higher modulus of the organic phase near the organic-inorganic interface and localized platelet-platelet contact can result in the observed elastic properties of nacre.

1. Introduction

Nacre, an important biological hard tissue has been of great interest recently due to its exceptional mechanical properties [1–15]. Biomimetic design [16–20] for the design of advanced laminated composites with optimized mechanical properties is of particular importance. The combination of suitable mechanical properties and environmentally benign processing routes makes the seashell structure very attractive and has led to recent advances in materials design inspired by biological origins.

Nacre is ceramic laminated composite consisting of highly organized polygonal shaped aragonitic platelet layers of thickness of 0.5 μm separated by thin 30 nm layers of organic composed mainly of proteins and polysaccharides. This particular microarchitecture is similar to 'brick and mortar' [1, 8, 9]. Such laminated microarchitecture is responsible for the high strength and fracture toughness of nacre. The portion of the nacre comprising the organic material typically represents 1–5% by weight. Microstructural characterization has shown the presence of a highly hierarchical morphology i.e., architectural order at many length scales, from nm to mm, not found in man-made systems [2, 3] The aragonitic structure also occurs in deposits of geologic origin and exhibits identical crystallographic structure but small differences are detected in the electronic structure possibly from the influence of organic [21].

Many engineered structures are designed and modeled using numerical modeling techniques, specifically finite element modeling (FEM). This is particularly true for modeling mechanical response of biological soft and hard tissues [22–24]. In this work, we construct the microarchitecture of nacre using finite element modeling techniques with microstructural parameters of size, shape etc obtained from previous work in literature. From the reported mechanical properties of

* Author to whom all correspondence should be addressed.

aragonitic platelets, geological aragonitic samples and organic matrix, simulated tests were conducted to predict mechanical properties of the 'composite'.

2. Formulation of finite element model of nacre

Finite element modeling is an important tool used by engineers to predict material properties based on discretization of the material into finite 'elements' that simulates the real continuous surroundings [25]. Often, complex tests and simulations can be conducted using FEM, which may be impossible or difficult to conduct in the laboratory. This is particularly true for biological systems. FEM is thus a commonly used tool in the biomaterials field for modeling heart, lung, bone etc. [22–24] In this work, we construct a 3D model of nacre. FEM software, MARC^{TM} (MSC MARC Corp.) was used on a silicon graphics workstation along with a pre and post processor, MENTAT^{TM} (MSC MARC Corp.)

As a first step, the individual 3D hexagonal aragonitic platelets were constructed based on microstructural parameters shown in Table I. Each aragonitic brick consisted of 4 eight noded isoparametric elements. The construction of a single element is shown in Fig. 1. Further, the organic layer was attached to all the faces of the aragonitic brick. The thickness of the organic layer was taken to be 0.015 μm which is half of the reported thickness of organic layer between aragonitic bricks. This constitutes the basic unit in the finite element analysis. Such a 3D element with both organic and inorganic phases was translated by 2.83 sin(π/3) μm nine times in the x direction to form a linear array of ten units. Fig. 2 shows such an array. This linear array was further translated in the x direction through 1.415 sin(π/3) μm and in the y direction by 2.1225 sin(π/3) μm. This leads to the staggering of bricks as seen in nacre. These two rows were then translated by 2.1225 μm in the y direction four times to yield a single layer of 10×10 units as shown in Fig. 3. Staggering of the bricks in the z direction was accomplished by translating the 10×10 units in x and y directions by 1.415sin(π/3) and 1.415cos(π/3) μm respectively and translating in the z direction by 0.53 μm. Such a 3D construction is translated four times to yield a $10 \times 10 \times 10$ structure as shown in Fig. 4. Mechanical tests are simulated on such a structure.

TABLE I Microstructural parameters, composition and elastic properties of the components of nacre

Organic	Inorganic
Proteins and Polysaccarides [1]	Aragonitic $CaCO_3$
Volume % of Nacre: 5	Volume % of Nacre: 95
30 nm layers between and around aragonitic platelets	Hexagonal Platelets with 2.8 μm sides and 0.5 μm height.
Elastic Modulus: 5 MPa [25]	Elastic Modulus: 205 GPa [1, 25]

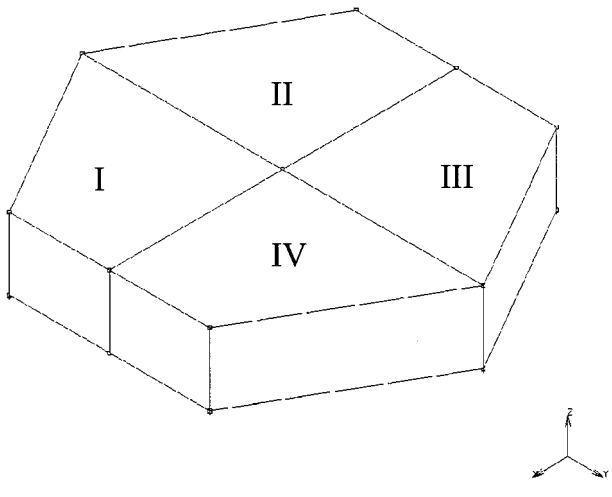

Figure 1 Construction of aragonitic brick from 4 isoparametric 3D elements labeled 1, 2, 3, and 4.

2.1. Material parameters

Elastic behavior of the whole shell is modeled using the elastic modulus for the individual components from literature, [1, 26] as shown in Table I. In literature, the elastic modulus of the organic layer is estimated using nano indentation techniques [26].

2.2. Boundary conditions

Tensile and compression tests were simulated by setting nodal displacements of the first or lowest face of the 3D model to zero and applying face pressure in the z direction to the top face of the 3D model. These boundary conditions were applied directly to aragonite surfaces. All the nodal displacements on the top aragonite face were equalized by linking all surface nodes to central node. This procedure effectively minimizes the 'edge effect' commonly observed in FEM analyses. In our analysis, as a first approximation, no interphasial, i.e. pertaining to discrete interphase, relationships between organic – inorganic phases were introduced. The inorganic-organic interface is assumed to have perfect molecular adhesion and failure of nacre is attributed mainly to weakening of cohesive interactions in aragonite and nacre. This is a valid assumption since all tests were conducted well within the elastic regime. The specific role of interphase and weak interactions between organic and inorganic layers is addressed in subsequent work.

3. Results and discussion

Tensile tests were conducted with single load increment of 2×10^{-6} N/μm^2 (2 MPa). This load was estimated to occur well within the elastic range based on the experimental data from literature [1]. The reported mechanical behavior results in yield strength of 56×10^{-6} N/μm^2 (or 56 MPa). The resulting displacements of elements are shown in Fig. 5. A section of the simulation in the x-z plane is shown in Fig. 6. For the $10 \times 10 \times 10$ element constructed, the net displacement in the z direction was observed to be 0.9499 μm which corresponds to an elastic modulus of the whole shell to be 0.011 GPa as shown in Table II. The reported modulus in literature is 25–50 GPa [1]. The origin of the three orders of magnitude discrepancy arises from the

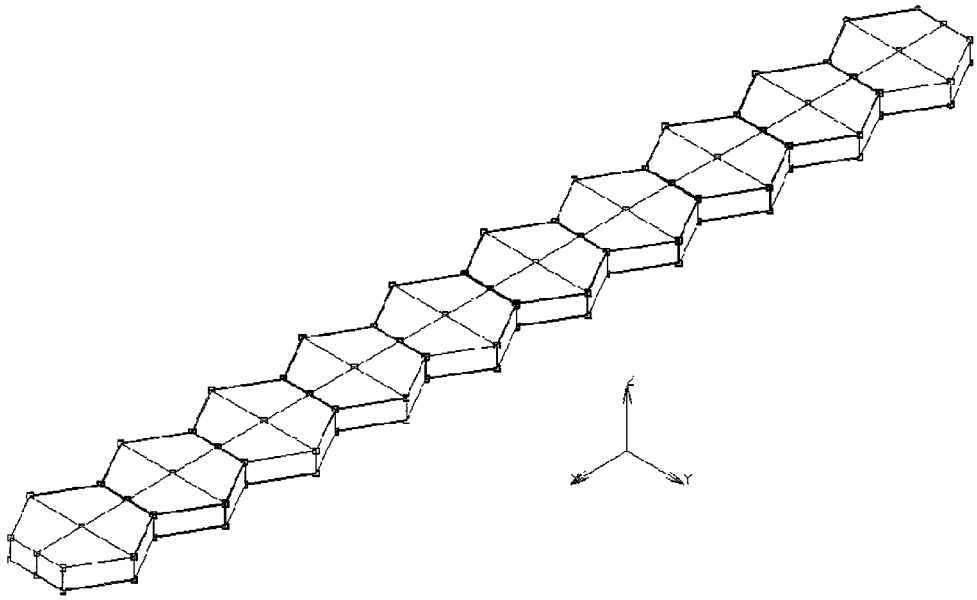

Figure 2 Linear array of ten elements of aragonite with organic layer.

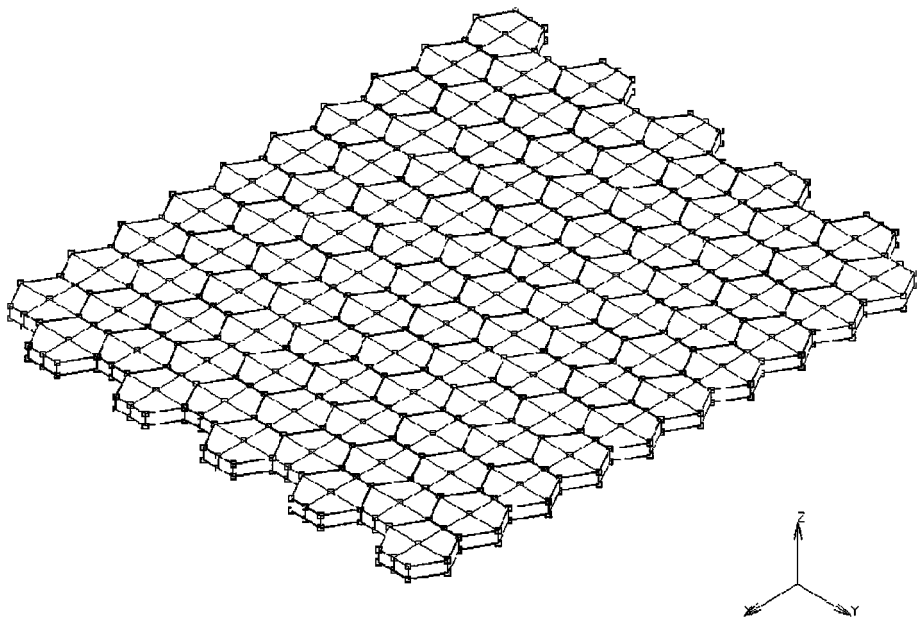

Figure 3 Single layer of 10×10 organic-inorganic units.

TABLE II Displacements observed in simulated tensile tests at 2 MPa single load increment and corresponding elastic moduli

Displacement (μm)	Total Strain (%)	Elastic Modulus (GPa)
9.499E-1	18.02466	0.011
4.473E-4	0.00849	23.557
1.05E-4	0.00199	100.503

extremely low modulus of the organic phase reported in literature using nanoindentation experiments [26]. Molecular analysis of the organic phase [27] has shown a layered morphology exhibited by the organic phase with several layers, each showing a different molecular composition and arrangement and thus with unique mechanical properties. The reported modulus of the organic layer is thus representative of only a thin section of the organic phase. Thus the composite modulus of the organic phase is possibly continuously changing across its thickness. The elastic modulus of the composite organic layer maybe substantially higher. In our effort to model the net modulus of the organic phase, we used the reported modulus of the whole shell and varied the modulus of the organic phase from 0.005 GPa to 15 GPa. The displacements at 15 GPa are shown in Fig. 7. A section of the simulation in the x-z plane is shown in Fig. 8. For a $10 \times 10 \times 10$ element, the net displacement was observed to be 4.473×10^{-4} μm. This displacement corresponds to an elastic modulus of 23.6 GPa as shown in Table II. This value agrees well with the reported modulus of the organic phase. Thus, our FEM analysis indicated that the average modulus of the organic interphase is of the order of 15 GPa.

Another possible explanation for the large displacements and hence extremely low modulus of nacre as shown in the simulations could possibly result from

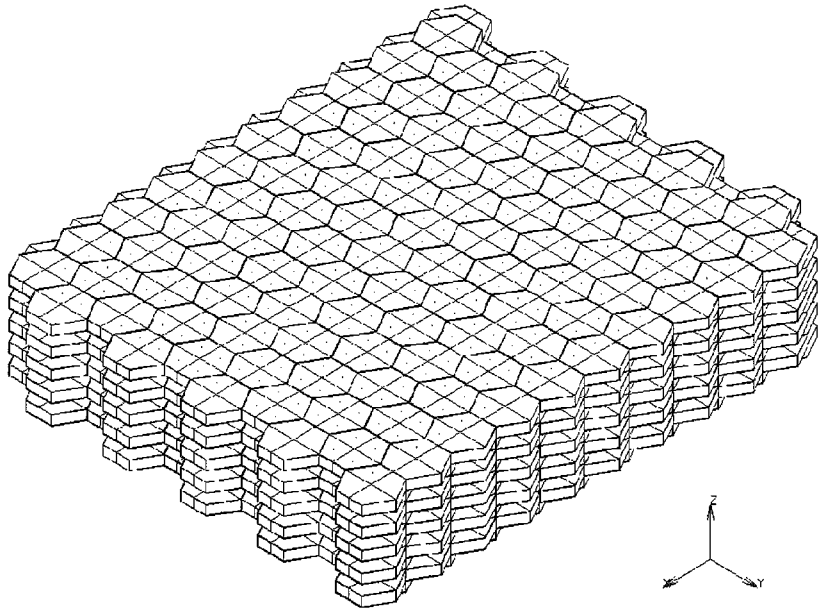

Figure 4 Three dimensional construction of $10 \times 10 \times 10$ organic-inorganic units.

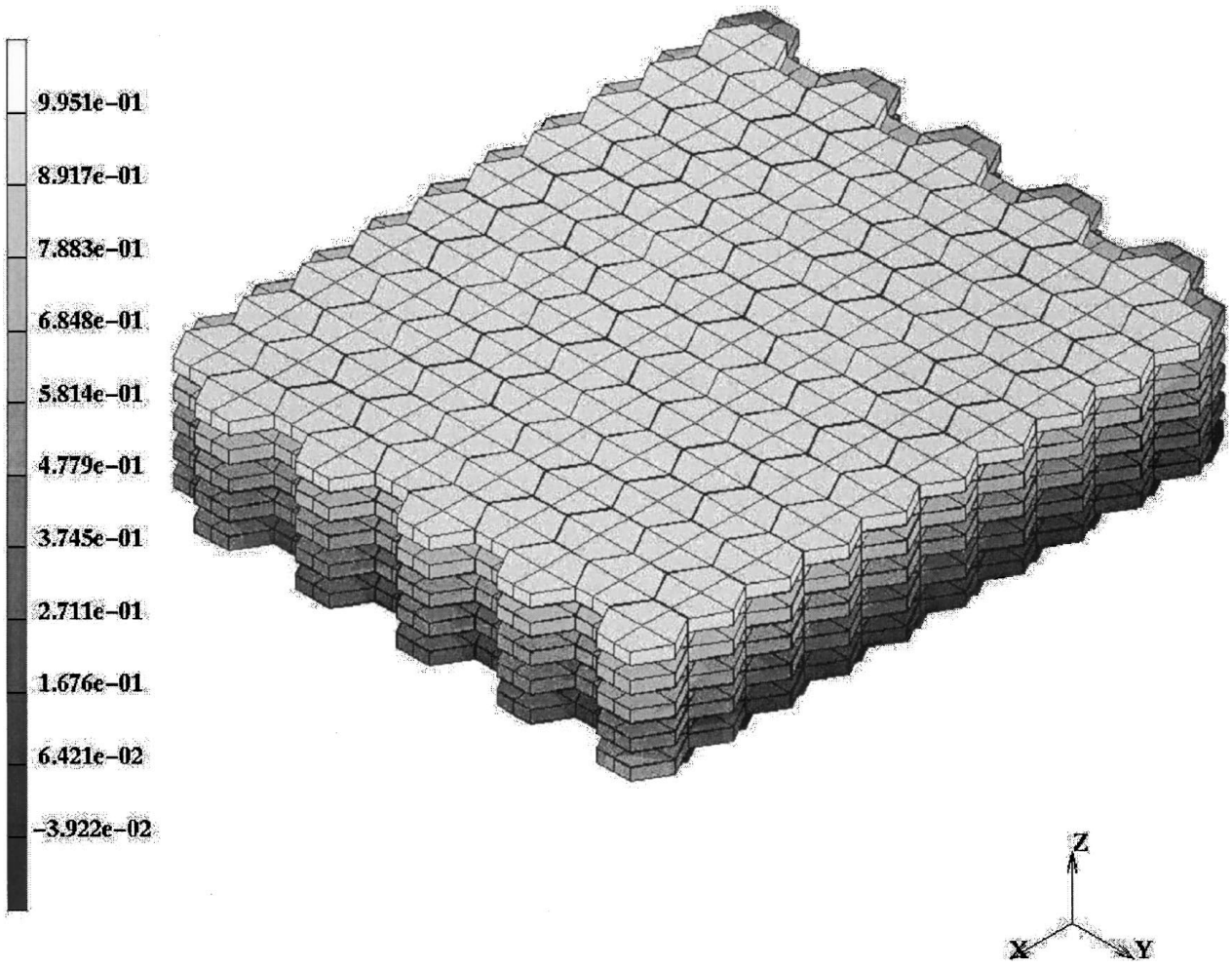

Figure 5 Contour band plots of displacements under simulated tensile test (Single load increment = 2 MPa, Elastic modulus of organic = 0.005 GPa). Grayscale legend corresponds to displacements in z direction in μm.

a localized aragonite-aragonite contact between the platelets. Such contacts can substantially reduce the displacements due to the high modulus of the aragonitic phase. Simulation using the same model for complete absence of organic interlayers resulted in a net displacement of 1.05×10^{-4} μm. As shown in Table II this corresponds to an elastic modulus of 100 GPa.

The third plausible situation is a combination of the above two, i.e. a higher composite modulus of the

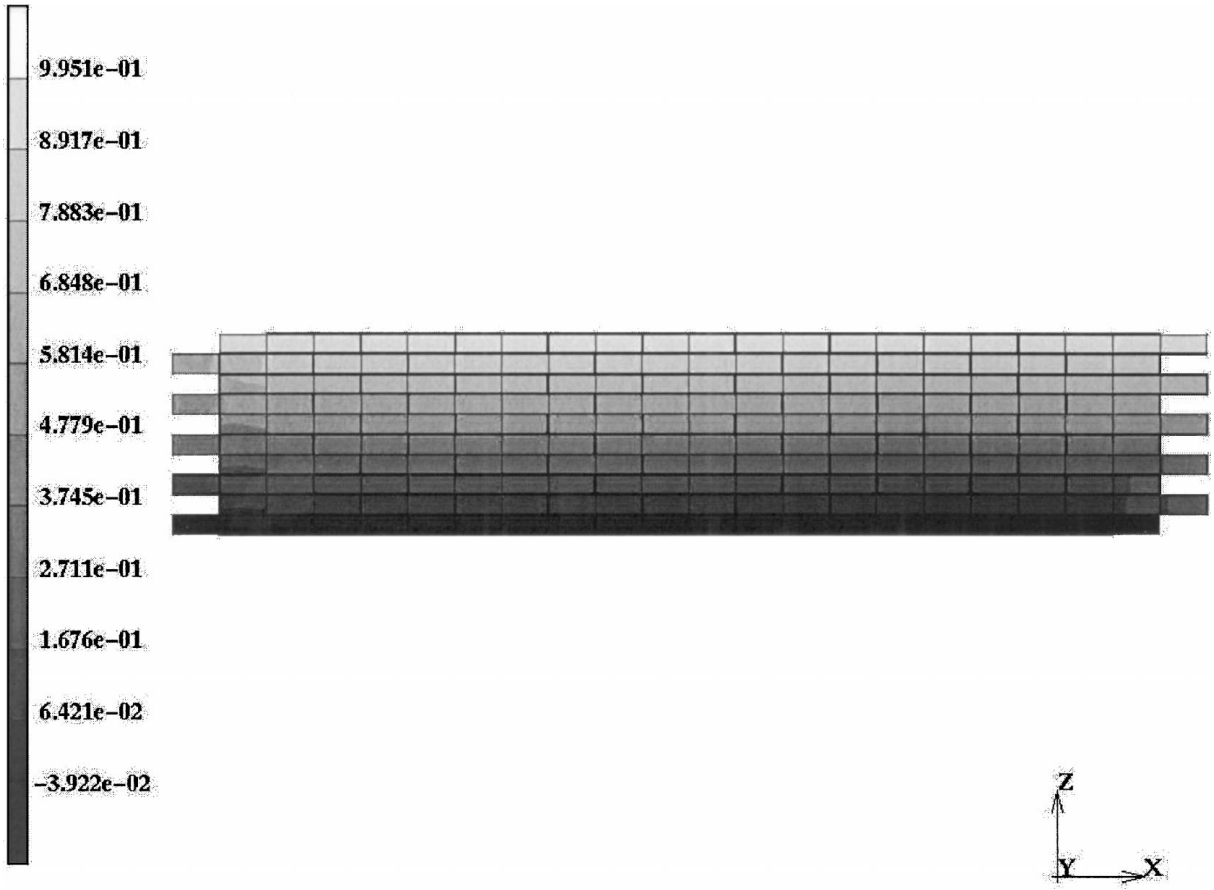

Figure 6 A section through the center of the simulations shown in Fig. 5 in the *x*-*z* plane. Grayscale legend corresponds to displacements in *z* direction.

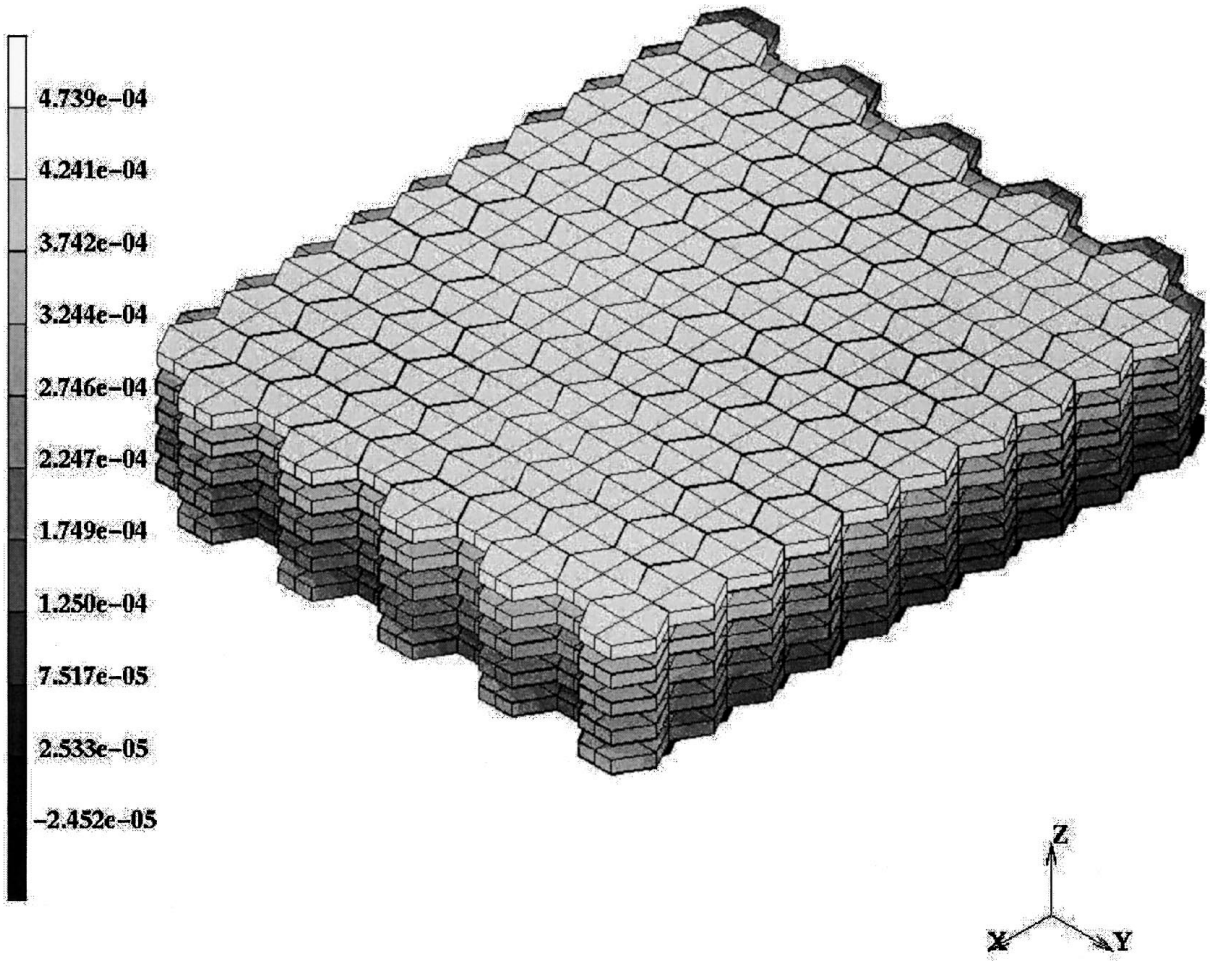

Figure 7 Contour band plots of displacements under simulated tensile test (Single load increment = 2 MPa, Elastic modulus of organic = 15 GPa). Grayscale legend corresponds to displacements in *z* direction in μm.

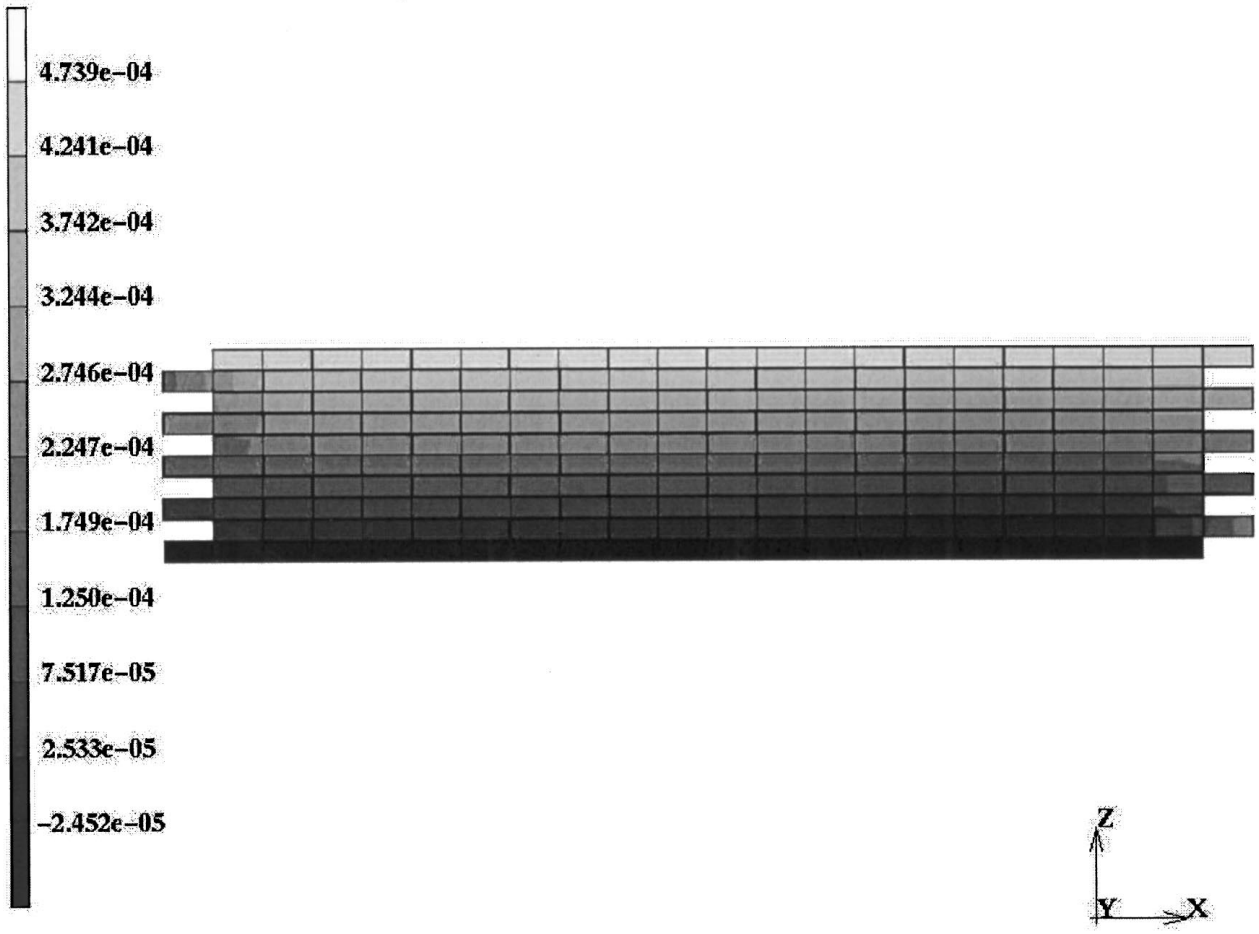

Figure 8 A section through the center of the simulations shown in Fig. 7 in the x-z plane. Grayscale legend corresponds to displacements in z direction in μm.

organic phase and direct transfer of load between a portion of aragonitic platelets.

4. Conclusions

A 3D finite element model has been constructed for nacreous structure using the reported material and microstructural parameters from literature. Tensile tests were simulated using this model. The tests were conducted at low stresses of 2 MPa. These stresses occur well within the elastic regime of nacre and thus effects related to locus and extent of damage were ignored. Our simulations showed that using the reported values of moduli of organic and aragonitic platelets, the displacements observed were extremely large and correspond to a very low modulus of 0.011 GPa for nacre. Since this value is about three orders of magnitude lower than the reported modulus of nacre, three possibilities are suggested:

i. We estimate that the actual modulus of the organic layer is much higher than that reported. This can arise from the multilayer structure of the organic phase with each layer exhibiting a different elastic modulus. To verify such a hypothesis, we conducted simulated tensile tests using the constructed FEM 3D model of nacre with varying modulus of the organic phase from the reported value of 0.005 GPa to 15 GPa. Our results using the organic elastic modulus as 15 GPa yield an elastic modulus of 23.6 GPa for nacre. This value is consistent with that reported from literature. Thus our simulations suggest that the average elastic modulus of the organic layer in nacre be of the order of 15 GPa.

ii. Aragonitic platelet contact in nacre can result in reduced displacements and thus a higher modulus. Simulations using a complete absence of organic phase yield a modulus of 100 GPa.

iii. Another scenario is a combination of the above two, wherein a higher modulus of the organic phase in combination with platelet-platelet contact in a fraction of the inorganic phase yields the observed elastic behavior of nacre.

Further, as more information on the molecular level processes at the organic-inorganic interface and molecular structure and properties of the organic layer are revealed, complex tests can be simulated using the FEM model of nacre which may not be feasible in the laboratory. These simulations can help in developing new laminated composite materials mimicking the nacre microstructure. A comparison of FEM simulations with mechanical tests performed in the laboratory can thus shed light on nature of mechanical behavior at interfaces in complex biological systems.

Acknowledgements

The authors acknowledge National Science Foundation (Visualization Project #9512547) and Dr. K. Ebeling for

computational facilities. ND EPSCoR (Project #8301) is acknowledged for acquisition of MARC finite element analysis software.

References

1. J. D. CURREY, in "The Mechanical Properties of Biological Materials," edited by J. F. V. Vincent and J. D. Currey (Cambridge University Press, London, 1980) p. 75.
2. M. SARIKAYA and I. A. AKSAY, in "Structure, Cellular Synthesis, and Assembly of Biopolymers," edited by S. Case (Springer-Verlag, Berlin, 1995) p. 1.
3. A. P. JACKSON, *J. Mater. Sci. Lett.* **5** (1986) 975.
4. A. H. HEUER, D. J. FINK, D. J. LARAJAI, J. L. ARIAS, P. D. CALVERT, K. KENDALL, G. L. MESSING, J. BLACKWELL, P. C. RIEKE, D. H. THOMPSON, A. P. WHEELER, A. VEIS and A. I. KAPLAN, *Science* **255** (1992) 1098.
5. K. SIMKISS and K. M. WILBUR, in "Biomineralization: Cell Biology and Mineral Deposition" (Academic Press, New York, 1989) p. 231.
6. P. CALVERT, *MRS Bull.* **10** (1992) 37.
7. *Idem., Mater. Res. Soc. Symp. Proc.* **180** (1990) 619.
8. M. YASREBI, G. H. KIM, K. E. GUNNISON, D. L. MILIUS, M. SARIKAYA and I. A. AKSAY, *Mat. Res. Soc. Proc.* **180** (1990) 625.
9. M. SARIKAYA, K. E. GUNNISON, M. YASREBI, D. L. MILIUS and I. A. AKSAY, *Mat. Res. Soc. Proc.* **174** (1990) 109.
10. J. LIU, M. SARIKAYA and I. A. AKSAY, *ibid.* **255** (1992) 9.
11. A. P. JACKSON, J. F. V. VINCENT and R. M. TURNER, *Proc. R. Soc. Lond.* **B234** (1988) 415.
12. S. MANN, in "Biomineralization: Chemical and Biological Perspectives," edited by S. Mann, J. Webb and R. J. P. Williams (VCH Verlagsgesselschaft, Weiheim, 1989) p. 35.
13. R. Z. WANG, H. B. WEN, F. Z. CUI, H. B. ZHANG and H. D. LI, *J. Mater. Sci.* **30** (1995) 2299.
14. J. F. V. VINCENT, "Structural Biomaterial" (MacMillan Press, London, 1982) p. 171.
15. M. SARIKAYA and I. A. AKSAY, "Design and Processing of Materials by Biomimetics" (American Institute of Physics, Washington D.C., 1995) p. 1.
16. A. M. BELCHER, X. H. WU, R. J. CHRISTENSEN, P. K. HANSAMA, G. D. STUCKY and D. E. MORSE, *Nature* **381** (1996) 56.
17. L. ADDADI and S. WEINER, *Agnew Chem. Int. Ed Engl.* **31** (1992) 153.
18. A. M. BELCHER, P. K. HANSAMA, G. D. STUCKY and D. E. MORSE, *Acta Materialia* **46** (1998) 733.
19. S. MANN, *Nature* **365** (1993) 499.
20. S. MANN, D. D. ARCHIBOLD, J. M. DIDYMUS, T. DOUGLAS, B. HEYWOOD, F. C. MELDRUM and N. J. REEVES, *Science* **261** (1993) 1286.
21. K. S. KATTI, M. QIAN, D. W. FRECH and M. SARIKAYA, *Microsc. Microanal.* **5** (1999) 358.
22. S. E. BORGERSEN and R. L. SAKAGUCHI, *ASME Int. Mech. Eng. Conf.* **28** (1994) 129.
23. G. W. BRODLAND and D. A. CLAUSI, *J. Biomech. Eng.* **116** (1994) 146.
24. K. K. MENDIS, R. L. STALNAKER and S. H. ADVANI, *ibid.* **117** (1995) 279.
25. C. S. DESAI and J. F. ABEL, "Introduction to the Finite Element Method" (Van Nostrand Reinhold, New York , 1972)
26. B. SHAPIRO, MS thesis, University of Washington, Seattle, 1996.
27. S. WEINER and W. TRAUB, *Phil. Trans. R. Soc. Lond. B* **304** (1984) 425.

Received 20 October 1999
and accepted 2 August 2000